Report No. 54-66

NASA CR71292

Thermo Electron Engineering Corporation, 85 First Avenue, Waltham, Massachusetts 02154

SECOND QUARTERLY PROGRESS REPORT

APPLIED THERMIONIC RESEARCH

This work was performed for the Jet Propulsion Laboratory, California Institute of Technology, sponsored by the National Aeronautics and Space Administration under Contract NAS7-100.

Contract 951262

25 September to 25 December, 1965

by

S. Kitrilakis
D. Lieb
F. Rufeh

Prepared for

Jet Propulsion Laboratory

Pasadena, California

Approved by S Kitrilakis

S. Kitrilakis
Research Manager

TABLE OF CONTENTS

LIST OF ILLUSTRATIONS

CHAPTER I

INTRODUCTION AND SUMMARY

The primary objective of this program is the study of two processes of Cs-vapor thermionic conversion. The first process uses cesium fluoride vapor in addition to metallic cesium to provide one additional degree of freedom in obtaining given electrode work functions. The second process uses an inert gas in addition to cesium. It is expected that, under proper conditions, the presence of the inert gas will aid in the conservation of ions generated in the interelectrode volume and thus reduce the internal voltage drop.

The experimental study of both schemes of thermionic conversion is divided into two classes of experiments. The first class of experiments is more basic in nature and consists primarily of determining the effect of the CsF and inert-gas additives on electrode work functions for the former, and on the plasma for the latter. The second class of experiments is the generation of parametric-type performance data over wide ranges of variation of converter parameters. The basic experiments precede the parametric studies, since it is expected that they will guide the selection of conditions which will optimize the effects of these additives. In parallel with the experimental programs outlined above, analytical and correlation work is conducted, its objective being the formulation of valid physical models and the quantitative description of the processes.

The cesium fluoride additive work is a direct continuation of the program of the previous year under JPL Contract No. 950671/NAS7-100. The program demonstrated very impressive performance with CsF, which, however, could not be maintained over long periods of time. A specific objective of the present work is to obtain the enhanced performance in a stable manner and then define it parametrically over a wide range.

The inert gas "plasma additive" concept is an outgrowth of the analytical work done in the previous year under the contract named above.

In the course of this quarter, considerable effort was devoted to the analysis associated with the two experimental tasks described above. An analytical treatment of the Boltzmann region of the current voltage characteristic is presented in Chapter II. This region received special attention because of its importance in the measurement of collector work function and its key role in understanding lower mode operation. The results of the theoretical work were in good agreement with experimental data and the procedure of collector work function measurement developed should prove very useful.

The experimental data generated with inert gases in converters is of little value unless some sort of analytical framework is available to guide the interpretation of the data. Such a framework was developed and is presented in Chapter III. A significant result of this analysis is that inert gas injection can be a very powerful tool in the study of the plasma.

The analysis and correlation of surface additive data uncovered a very important property of the three component system: The effects of the additive and the cesium vapors are separable. This property and its significance are discussed in Chapter IV.

The emphasis in this report has been placed on the theoretical work conducted to date because this aspect of the program is now sufficiently advanced to serve in the interpretation of the experimental results now being generated. The third quarterly report will present extensive testing with experimental data of the partially tested hypotheses advanced here.

CHAPTER II

ELECTRON SCATTERING IN THE BOLTZMANN REGION

1. GENERAL

Analytical and experimental studies of the Boltzmann region of current voltage characteristics are presented in this chapter. This region is part of the unignited mode and has been defined[1] "as the region where the electrons from the plasma begin to reach the collector." Characteristic of this region is the fact that plasma electrons encounter a barrier consisting of the sum of the output voltage and collector work function. As a result, the number of electrons that surmount this barrier varies exponentially with output voltage.

The Boltzmann region has received a great deal of attention[2, 3, 4, 5] in experimental and theoretical studies because of its importance in the experimental determination of the collector work function and its key role in unignited mode operation. In spite of these efforts, however, a number of observations reported in the literature are in apparent conflict. It is the objective of this chapter to show that these observations can be accounted for if all the relevant phenomena are considered. In addition to the physical interpretation given, practical guidelines are furnished for the determination of accurate values of collector work function.

Any study of this region is hampered by the cesium ion current, generated by surface ionization at the emitter surface and accelerated toward the collector, which cannot be distinguished from the electron current. In this study this complication was avoided by conducting all experiments under highly electron rich conditions. In addition, the electron density was kept sufficiently small to render electron-electron interactions negligible. The dominant effect under these conditions was the scattering of electrons by cesium atoms. It was, therefore,

possible to study electron neutral collisions and to determine the mean free path of electrons in cesium vapor.

Two distinct modes of electron scattering exist depending on the ratio of electron mean free path, λ, to interelectrode spacing, d. When the electron mean free path is larger than the spacing, electrons which collide with a cesium atom and are deflected toward the emitter will most probably reach the emitter without suffering another collision and therefore have very small chances of reaching the collector. Conversely, when the mean free path is smaller than the spacing, the electrons that are deflected toward the emitter stand a good chance of suffering additional collisions and, therefore, have much greater probability of reaching the collector.

The above qualitative considerations make it necessary to differentiate between these two cases, both analytically and experimentally, as was done in the present work. Nevertheless, the scattering cross sections obtained in the two cases must be in agreement if the model postulated is correct.

2. THEORY

The Boltzmann mode of operation being considered here is characterized by the fact that the barrier composed of the collector work function and output voltage is greater than the emitter work function barrier (Figure II-1). If in addition the electron current emitted by the collector and the emitter ion current are negligible, and the emitted electrons suffer no collision, of any kind, then the output current is given by the Richardson equation:

$$J_o = A T_E^2 \exp\left[-(\phi_C + eV)/kT_E\right] \qquad (1)$$

where:

$A \equiv$ Richardson constant

$T_E \equiv$ Emitter temperature

$\phi_C \equiv$ Collector work function

$V \equiv$ Voltage output

$k \equiv$ Boltzmann constant

$e \equiv$ Electronic charge

The effect of electron scattering by cesium atoms shall be deduced from the deviation of the actual current from that predicted by equation (1). This analysis is based on the following assumptions:

1. Ion current and back-emission are negligible compared to the net electron current.
2. The electrons can be divided into two groups depending on whether their energies are larger or smaller than $(\phi_c + eV)$ and can be treated separately.

To satisfy the first assumption, the emission must be highly electron rich and the collector temperature sufficiently low so that back emission is negligible. The second assumption has been suggested by Hansen and Warner[2] and is justified in this analysis since, for $\beta < 1$, the electron density is sufficiently low to render electron-electron interactions negligible.

Only the fraction of electrons that possess energies larger than $(\phi_C + eV)$ need be considered, since the others will not be able to surmount this barrier and will be returned to the emitter without interacting with any part of the system. The number of these more energetic electrons, J_o, is given by equation (1). Of these a smaller number J will reach the collector, and the remainder will be scattered back to the emitter. J is related to J_o by a probability factor, S:

$$J = SJ_o \tag{2}$$

The probability S will be evaluated for the long- and short-mean-free-path cases.

a. Long-Mean-Free-Path Solution; $d/\lambda << 1$

In the region where the interelectrode spacing is smaller than electron mean-free-path, the incremental change in the directional electron current, dJ, in the interval x to x + dx is given by:

$$dJ = J\Sigma\omega dx \tag{3}$$

where:

$J \equiv$ electron current

$\Sigma \equiv$ macroscopic cross section $= N\sigma$

$N \equiv$ cesium atom density

$\sigma \equiv$ microscopic collision cross section of electrons with cesium atoms

$x \equiv$ distance

and ω is the fraction of particles scattered from an elastic sphere that have a component of velocity in the negative x direction, i.e., ω is the fraction of the projected area of the sphere that reflects the incident particles by more than 90°. From geometrical considerations:

$$\omega \equiv [\sin(\pi/4,)]^2 = \tfrac{1}{2} \tag{4}$$

Integrating equation (1) from x = o to d

$$J = J_o \exp(-d/2\lambda) \tag{5}$$

where λ is the electron mean free path in cesium vapor and is given by

$$\lambda = \frac{1}{N\Sigma} \tag{6}$$

Comparison of equations (1) and (5) shows that when $d/\lambda < 1$ the effect of electron scattering by neutrals is to reduce the output current by a constant fraction, $\exp(-d/2\lambda)$. In a plot of lnJ versus V this amounts to a translation of the J-V characteristic along the voltage axis. If J is used in equation (1) instead of J_o, an apparent collector work function, ϕ_{ca}, is computed as in equation (7):

$$J = AT_\epsilon^2 \exp(\phi_{ca} - eV)/kT_\epsilon \qquad (7)$$

The difference between the actual and apparent collector work functions, $\Delta\phi_c$, is given by:

$$\Delta\phi_c = \phi_{ca} - \phi_c = \frac{kT_\epsilon}{2\lambda} d \qquad \text{for } d/\lambda < 1 \qquad (8)$$

Equation (8) gives the deviation of the measured collector work function, ϕ_{ca}, from its true value ϕ_c as a function of interelectrode spacing d, electron mean-free-path λ and emitter temperature T_ϵ for $d/\lambda < 1$.

b. Short-Mean-Free-Path Solution, $d/\lambda >> 1$

In this region again only the more energetic electrons need be considered. The motion of electrons in the interelectrode space in this case is characterized by many collisions with neutral atoms which result in the randomization of their direction. In effect, their motion is diffusion dominated. For an absorption free diffusing medium the diffusion equation is of the form:

$$\nabla^2 n = o \qquad (9)$$

where n is the electron density. The boundary conditions are:

At the emitter $\qquad \frac{vn}{4} - \frac{1}{2} D \nabla n = J_o \qquad (10)$

At the collector $\qquad \frac{vn}{4} + \frac{1}{2} D \nabla n = o \qquad (11)$

where:

v ≡ average electron velocity

D ≡ electron diffusion coefficient in cesium vapor

The first boundary condition states that, at the emitter boundary of the plasma, the directional current into the plasma is equal to J_o, i.e., J_o fast electrons enter the plasma from the emitter. The second boundary condition states that the directional current into the plasma at the collector boundary is zero. The solution to the differential equation is given by:

$$n(x) = C_1 x + C_2 \tag{12}$$

From the two boundary conditions, the constants C_1 and C_2 are found to be

$$C_1 = \frac{-4 J_o}{4D + vd} \tag{13}$$

$$C_2 = \frac{4 J_o}{D} \left[\frac{2D + vd}{4D + vd}\right] \tag{14}$$

or

$$n(x) = \frac{-4 J_o}{4D + vd} \; x + \frac{4 J_o}{D} \left[\frac{2D + vd}{4D + vd}\right] \tag{15}$$

The net electron current J through the plasma is required by Fick's law to be

$$J = -D \frac{dn}{dx} \tag{16}$$

or

$$J = \frac{4 J_o D}{4D + vd} \tag{17}$$

The diffusion coefficient D is related to electron mean free path by

$$D = v\lambda/3 \tag{18}$$

Equations 17 and 18 give

$$\frac{J}{J_o} = \frac{1}{1 + \frac{3d}{4\lambda}} \tag{19}$$

Algebraic manipulation of equations (1) and (19) results in

$$J = A T_\varepsilon^2 \exp\left[-\frac{\phi_c + V + kT_\varepsilon \ln(1 + \frac{3d}{4\lambda})}{kT_\varepsilon}\right] \tag{20}$$

It follows from equation (19) that the effect of electron scattering is to translate the J-V curve along the voltage axis by the amount

$$kT_\varepsilon \ln(1 + \frac{3d}{4\lambda}) \tag{21}$$

The collector work function can be computed using the actual current J in equation (7) provided the apparent collector work function value, ϕ_{ca}, is corrected by $\Delta\phi_c$ as given by equation (22):

$$\Delta\phi_c = \phi_{ca} - \phi_c = kT_\varepsilon \ln(1 + \frac{3d}{4\lambda}) \tag{22}$$

3. EXPERIMENTAL TECHNIQUE AND RESULTS

In the preceding section on theoretical analysis it was shown that in the Boltzmann region the current voltage characteristic is exponential in voltage and displaced from the "idealized" Boltzmann line by a voltage increment which is a function of the spacing to mean-free-path ratio, d/λ.

The experimental technique chosen to test this hypothesis consists of measuring the change in apparent collector work function as a function of interelectrode spacing and cesium pressure.

A necessary condition for the success of this technique is that the emitter, collector and cesium reservoir temperatures remain constant while the spacing is varied. To accomplish this, an experimental procedure was developed which produces a direct measure of the change in the apparent collector work function as a function of spacing. This technique is based on the fact that in the Boltzmann region, where lnJ is proportional to output voltage, the effect of a spacing change is to translate the J-V characteristic along the voltage axis. Instead of generating a series of volt-ampere characteristics at different spacing settings, with the possibility that changes in the values of other parameters may take place, the output voltage is recorded as a function of spacing at constant output current. Changes in output voltage under these conditions are equal to the changes in the effective collector work function.

Two modifications of the variable parameter test vehicle[6] were necessary for the present experiment. First, the variable-spacing mechanism was equipped with a reversible electric motor so that the spacing could be varied continuously and at a constant rate from "minimum" to 60 mils. Second, an electric signal proportional to spacing was generated by using a 10-turn potentiometer driven by one of the micrometer screws that adjust the spacing. The emitter temperature was continuously monitored by a thermocouple. The diode and these changes are shown schematically in Figure II-2.

A typical run consists of varying the spacing while the electron current is kept constant at a selected value on the Boltzmann line, usually 1 mA. The output voltage is plotted as a function of spacing by an X-Y recorder, and the entire run is completed within a few seconds.

To investigate the long- and short-mean-free-path cases, two sets of data were taken, both covering a cesium temperature range of 510°-600°K (0.2-4.0 torr), at T_E = 1300°K. In the first set, the spacing was increased from minimum to several mils. In the second set, the spacing was decreased from 60 mils to minimum. Several typical runs for the two sets are shown (Figures II-3 - II-6 and Figure II-7). The reason for this procedure is that, for the first set, of primary interest was the spacing range of 0 - 5 mils; and it was important to minimize the departure from the state of equilibrium established prior to the run, whereas for the second set the larger spacings were of interest and the procedure was reversed.

4. COMPARISON OF EXPERIMENTAL RESULTS WITH THEORY

According to equation (8), for small spacings, $\Delta\phi_c$ is a linear function of the interelectrode spacing. The experimental data (Figures II-3 - II-6) show such a dependence. The slopes of the dashed lines were used to calculate the electron mean-free-path which is plotted as a function of inverse pressure (indicated by the diamonds) in Figure II-10.

The data from the high spacing range should fit equation (12); i.e., a plot of $\exp[\Delta\phi_c/kT_E]$ vs. spacing should be a straight line with the slope $\frac{3}{4\lambda}$. Such plots are shown in Figures II-8 and II-9 for two cesium pressures. The lower-pressure run (Figure II-8) agrees well with the form of equation (12) for d > 35 mils. A small deviation is observed at lower spacings. A case where the deviation is larger is shown in Figure II-9. This is probably due to small changes in emitter temperature, since emitter heat loss by cesium conduction becomes more important at higher pressures. Although a curvature is present at high pressures, the maximum variation of the slope of these curves is not large. The electron mean-free-path was calculated from such plots and is shown as a function of inverse

pressure in Figure II-10. Scatter bars indicate the maximum variation in the slope.

The values of the electron mean free path obtained by the two methods are in satisfactory agreement with each other, and show the expected dependence on cesium pressure.

The best fit to the data (Figure II-10) corresponds to $P\lambda = \frac{kT_g}{e\sigma} = 1.6$ mil-torr for the gas temperature $T_g = 960°K$, or the electron-atom collision cross section $\sigma = 230\ (\mathring{A})^2$. Table II-1 compares the value of σ obtained here with values reported or estimated by others for the same region of electron temperature.

TABLE II-1[7]

COLLISION CROSS SECTION OF ELECTRONS WITH CS ATOMS

	$\sigma(\mathring{A})^2$
This work[a]	230
Warner and Hansen[a]	200
Merlin[a]	200
Nottingham[c]	400
Roehling[a]	90
Stone and Reitz[b]	160
Zollweg and Gottlieb[a]	400
Robinson[b]	480
Harris[a]	320
Flavin & Meyerand[a]	310

a = experimental

b = theoretical

c = estimated

As may be seen, the value of $\sigma = 230(\mathring{A})^2$ is quite close to the most probable value and falls within the range of uncertainty.

5. CONCLUSIONS

Experimental evidence has been obtained which strongly supports the analytical model presented. This simple model describes adequately the experimental observations provided extraneous effects are either eliminated or accounted for. Of particular importance is the fact that the short and long mean-free-path cases treated have yielded the same value of electron-neutral scattering-cross-section. The $230(\mathring{A})^2$ value obtained is in good agreement with values obtained in other experiments and by theoretical calculation.

A reliable method has been devised for the experimental determination of collector work function values. Figure II-11 is a plot designed to facilitate the correction of observed apparent collector work function values for the effect of interelectrode spacing and cesium pressure.

CHAPTER II

REFERENCES

1. Bullis, Hanson, Houston, Koskinen, Rasor and Warner, "Proceedings of Thermionic Conversion Specialists Conference", San Diego, 1965.

2. L. K. Hansen and C. Warner, "Report on Twenty-Fourth Annual Conference, Physical Electronics", Cambridge, 1963.

3. J. J. Houston, "Proceedings of Thermionic Conversion Specialist Conference", Gatlinburg, 1963.

4. J. D. Dunlop, II, "Proceedings of Thermionic Conversion Specialist Conference", Cleveland, 1964.

5. Breitwieser, "Proceedings of Thermionic Conversion Specialist Conference", Gatlinburg, 1963.

6. Kitrilakis, et al., "Final Report for the Thermionic Research Program", Report No. TE7-66.

7. J. M. Houston, "Proceedings of Thermionic Conversion Specialist Conference", Cleveland, 1964.

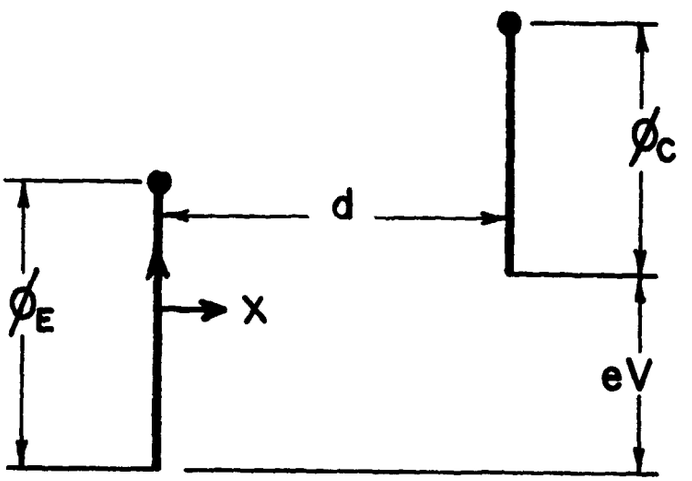

Figure II-1. Boltzmann Region

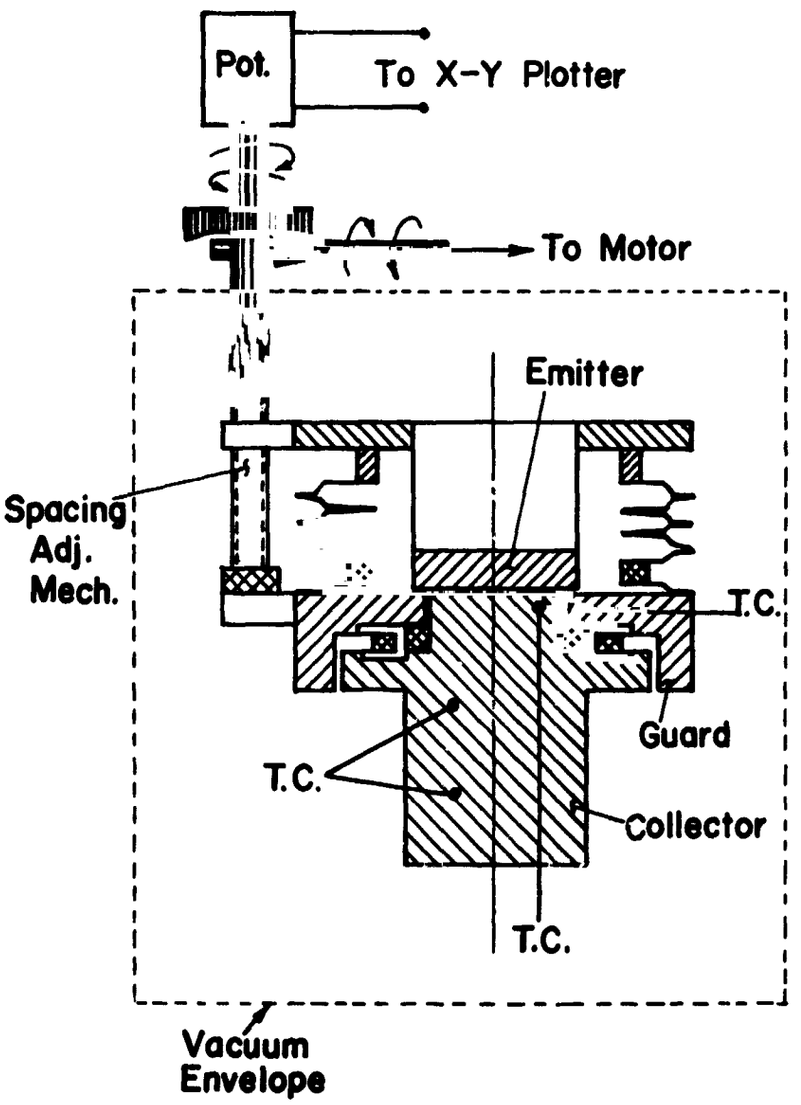

Figure II-2. Schematic of the Cesium Diode

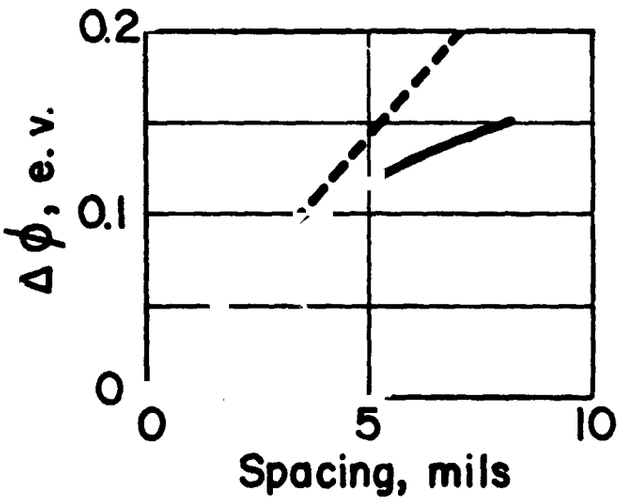

Figure II-3. Variation in Collector Work Function with Spacing.
T_E = 1314 °K, T_C = 609 °K, T_R = 543 °K.

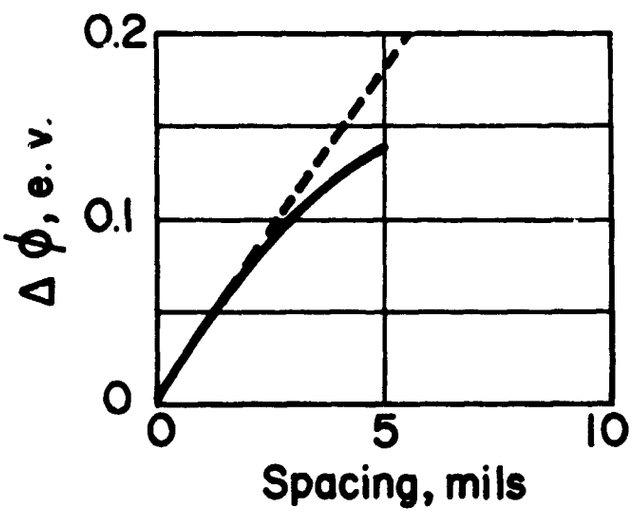

Figure II-4. Variation in Collector Work Function with Spacing.
T_E = 1313°K, T_C = 611°K, T_R = 554°K.

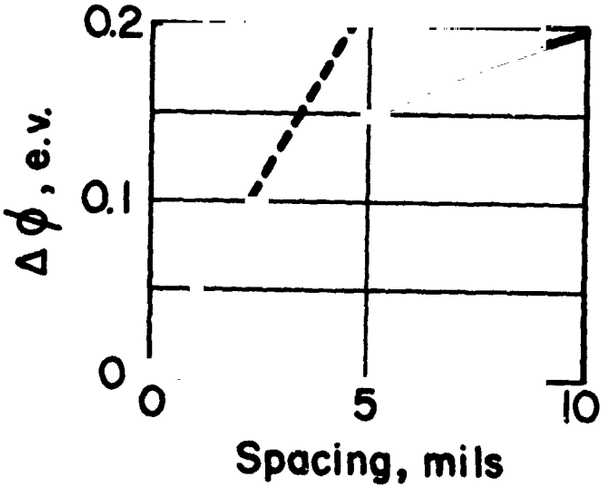

Figure II-5. Variation in Collector Work Function with Spacing.
T_E = 1298°K, T_C = 618°K, T_R = 572°K.

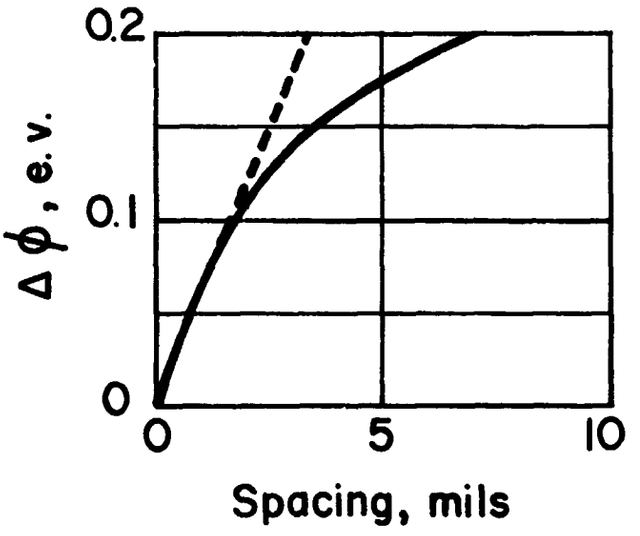

Figure II-6. Variation in Collector Work Function with Spacing.
T_E = 1308°K, T_C = 621°K, T_R = 593°K

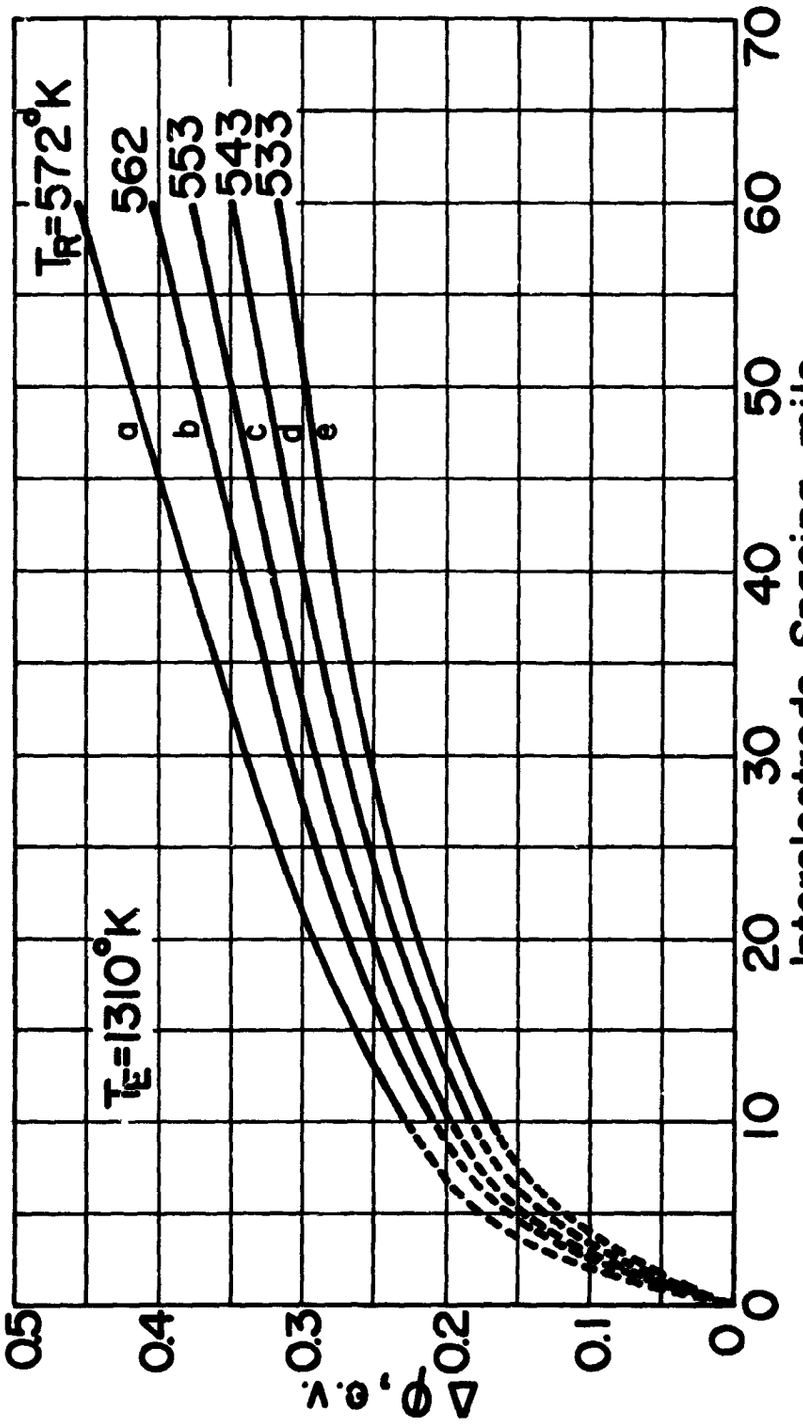

Figure II-7. Variation in Collector Work Function with Spacing.
(a) T_c = 628°K, (b) T_c = 628°K, (c) T_c = 627°K,
(d) T_c = 827°K, (e) T_c = 623°K.

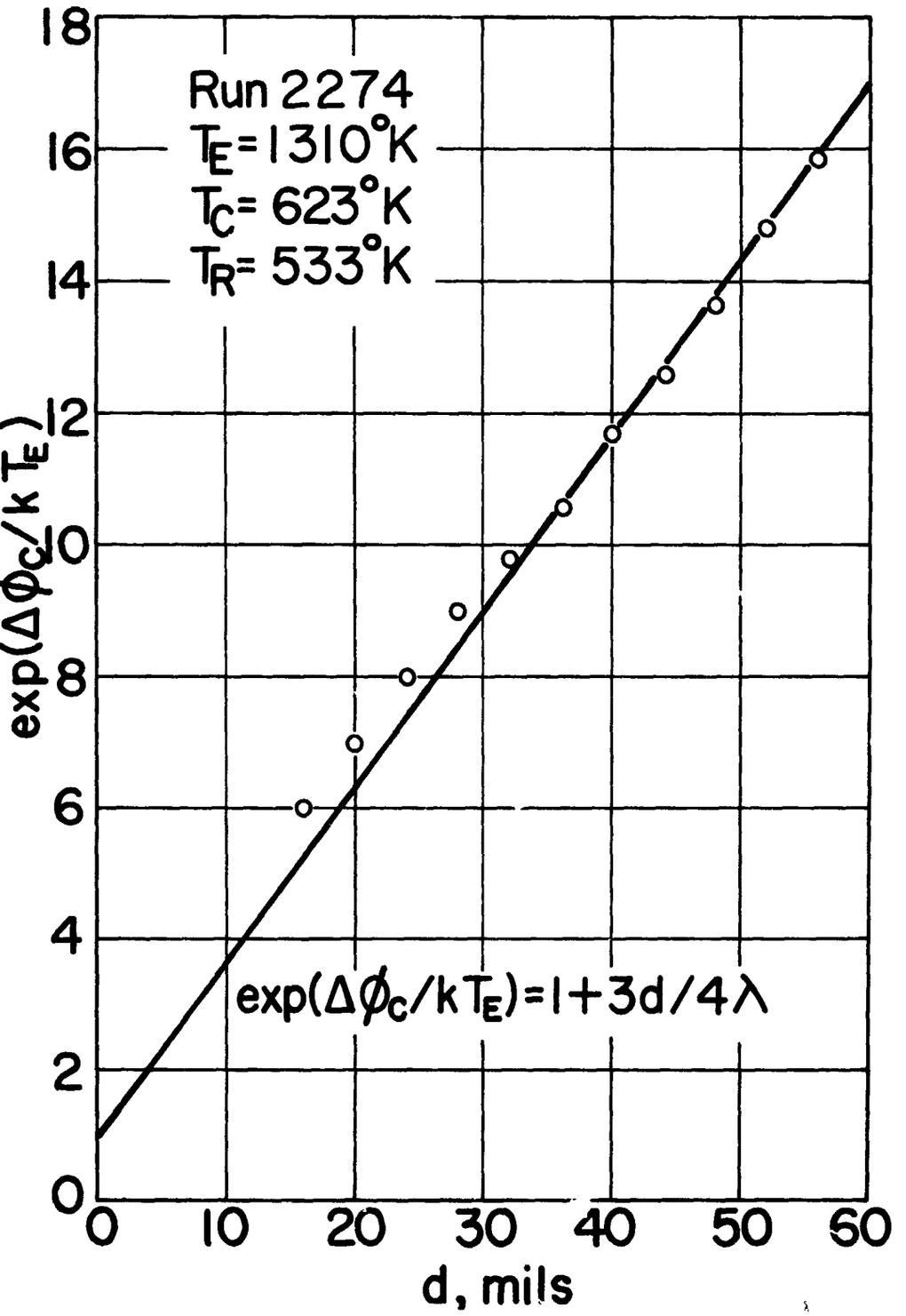

Figure II-8. Plot for Obtaining Electron Mean Free Path

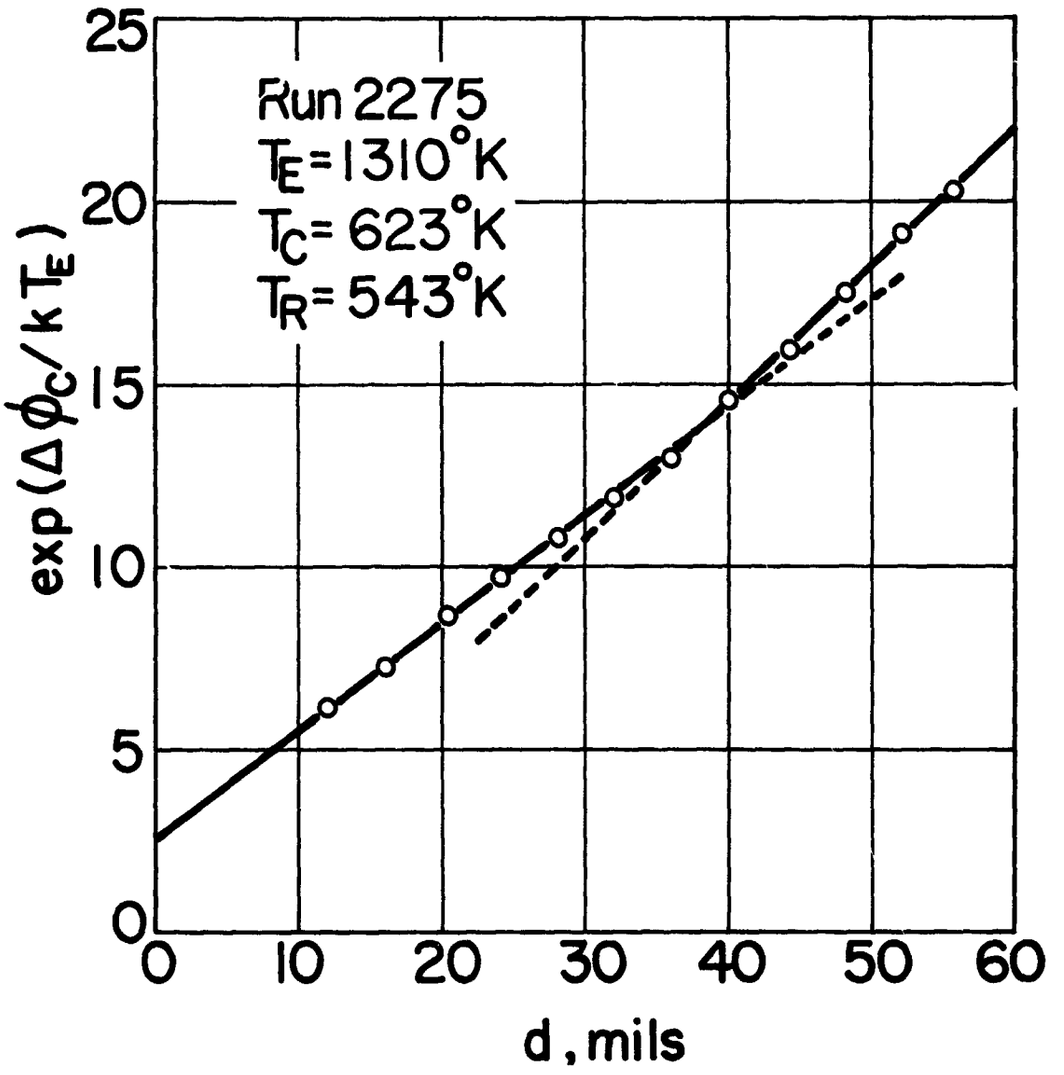

Figure II-9. Plot for Obtaining Electron Mean Free Path.

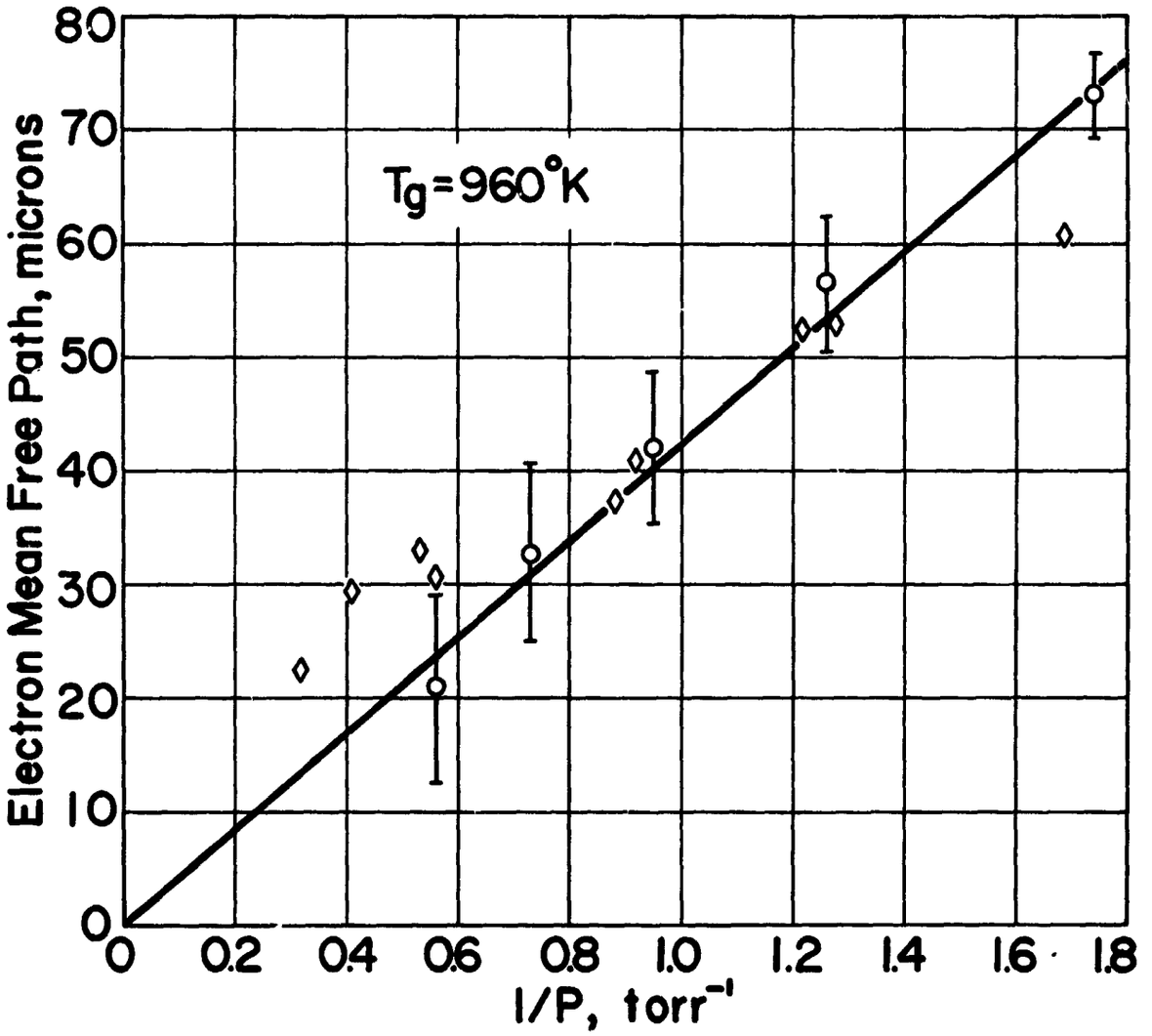

Figure II-10. Electron Mean Free Path in Cesium Vapor

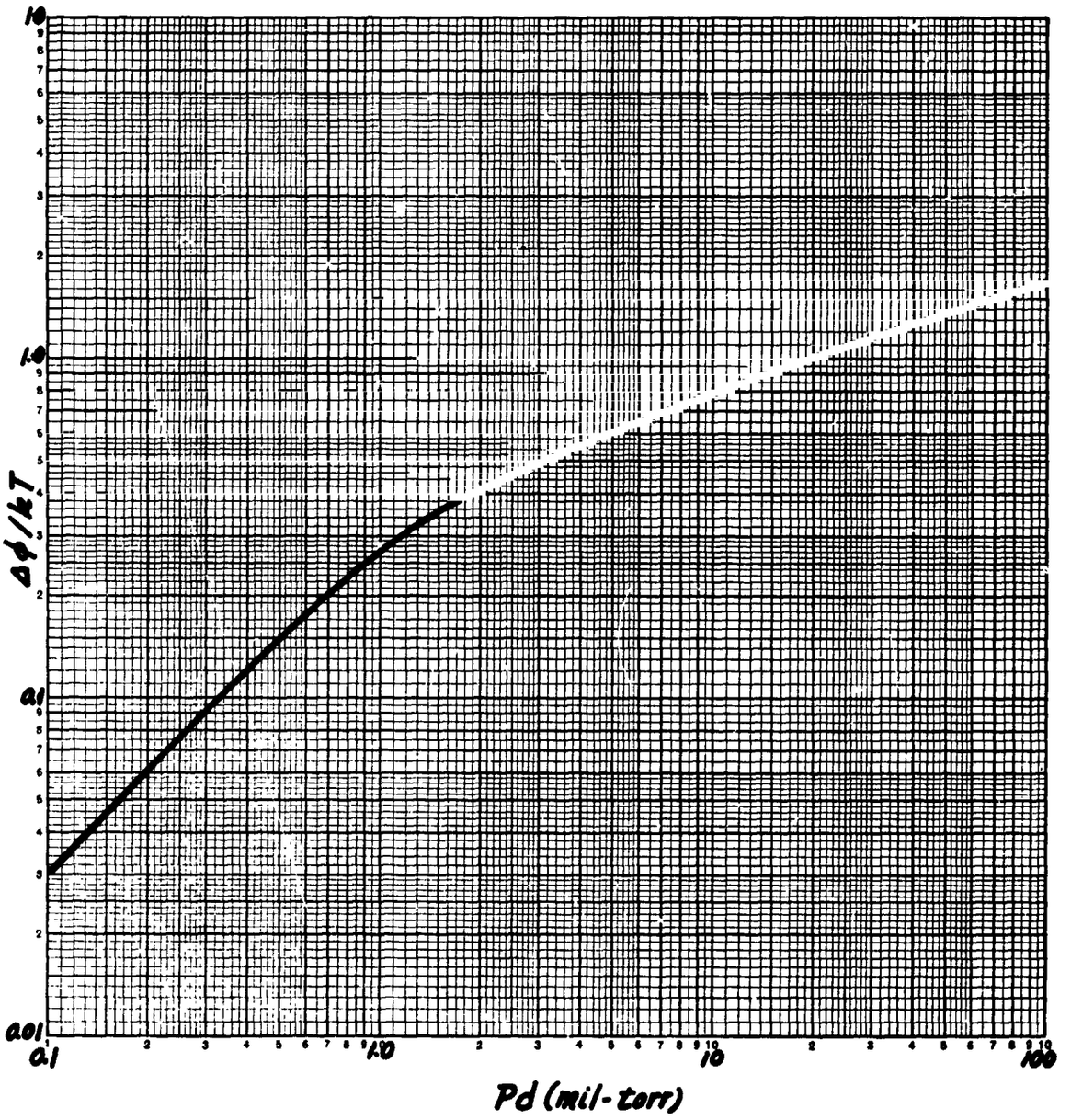

Figure II-11. Recommended Correction for Collector Work Function Measured by Retarding Technique.

CHAPTER III
INERT GAS STUDIES

1. GENERAL

The study of the effects of inert gases on the ignited mode constitutes a major portion of the experimental work in this program. The objective of that effort is to use the inert gas to prevent the diffusion of cesium ions toward the electrode walls where they are lost. To accomplish this objective, however, the hypotheses regarding the interactions of inert gases with the converter plasma must be tested experimentally.

An analytical treatment of the inert-gas-plasma interactions is given in this chapter followed by an outline of what are considered to be critical experiments, and are now in progress. Two aspects of the problem are given particular attention; the electron scattering by the combined vapors of cesium and argon, and the influence of argon on plasma parameters.

2. ELECTRON SCATTERING BY CESIUM AND ARGON

The process of electron scattering by neutrals is the dominant phenomenon in the "saturation" portion of the current voltage characteristic. It is, therefore, appropriate to study this process both analytically and experimentally in this region. The motive diagram for this mode of operation is shown in Figure III-1. The assumption will be made that the sheaths are of negligible thickness and the plasma neutral.

The transport of electrons through the plasma is governed by the diffusion equation which in a source-free-medium takes the form:

$$\nabla^2 n = o \qquad (1)$$

where n is the electron density. Equation (1) will be solved using the following boundary conditions:

$$\left[\frac{vn}{4} - \frac{1}{6}\frac{v}{\Sigma_1 + \Sigma_2}\frac{dn}{dx}\right] = J_s + \left[\frac{vn}{4} + \frac{1}{6}\frac{v}{\Sigma_1 + \Sigma_2}\frac{dn}{dx}\right]\left[1 - \exp\left(-V_E/kT_e\right)\right]$$

$$\text{at } x = 0 \qquad (2)$$

$$\frac{vn}{4} + \frac{1}{6}\frac{v}{\Sigma_1 + \Sigma_2}\frac{dn}{dx} = J_{cs} + \left[\frac{nv}{4} - \frac{1}{6}\frac{v}{\Sigma_1 + \Sigma_2}\frac{dn}{dx}\right]\left[1 - \exp\left(-Vc/kT_e\right)\right]$$

$$\text{at } x = d \qquad (3)$$

where

v ≡ average electron energy

Σ_1 & Σ_2 ≡ are the macroscopic scattering cross section of cesium and argon atoms respectively

J_s ≡ the emitter saturation current

T_e ≡ the electron temperature in the plasma

J_{cs} ≡ the collector saturation current

The first boundary condition states that the directional current in the positive x direction, at x = 0, is composed of the emitter saturation current, J_s, and the fraction of the directional current in the negative x direction that was reflected from the emitter sheath, V_E. The second boundary condition states that at x = d, the directional current in the negative x direction is equal to the collector emission, J_{cs}, plus the fraction of the current in the positive x direction that was reflected from the collector sheath, V_c.

This analysis assumes that the electron mean free path is much larger than the plasma width and that velocity distribution of the electrons is Maxwellian.

The solution to the differential equation is of the form:

$$n(x) = C_1 x + C_2 \tag{4}$$

where C_1 and C_2 are determined from the boundary conditions:

$$C_1 = \frac{J_{cs} \exp [V_c/kT_{ec}] - J_s \exp [V_E/kT_{eE}]}{\frac{v}{3(\Sigma_1 + \Sigma_2)}[\exp(V_c/kT_{ec}) + \exp(V_E/kT_{eE}) - 1] + \frac{d}{4}} \tag{5}$$

$$C_2 = 4J_s \exp (V_E/kT_{eE}) + [4 \exp (V_E/kT_{eE}) - 2] \frac{J_{cs} \exp (V_c/kT_{eE}) - J_s \exp (V_E/kT_{eE})}{\exp(V_c/kT_{ec}) + \frac{3(\Sigma_1 + \Sigma_2)d}{4v} - 1 + \exp(V_E/kT_{eE})} \tag{6}$$

where T_{eE} and T_{ec} are the electron temperatures at the emitter and collector ends of the plasma respectively. The net current through the plasma is required by Fick's law to be

$$J = \frac{v}{3(\Sigma_1 + \Sigma_2)} \frac{dn}{dx} \tag{7}$$

Combining equations (4), (5) and (7), we get

$$J = \frac{J_s \exp [V_E/kT_{eE}] - J_{cs} \exp [V_c/kT_{ec}]}{\frac{3d(\Sigma_1 + \Sigma_2)}{4v} + \exp [V_c/kT_{ec}] + \exp [V_E/kT_{eE}] - 1} \tag{8}$$

In equation (8) the net current through the plasma is given in terms of plasma parameters. To facilitate the comparison with experimental results this equation

will be simplified. The back emission from the collector is usually small and can be neglected subject to the following condition.

$$J_{cs} \ll J_S \exp\left[\frac{V_E}{kT_{eE}} - \frac{V_C}{kT_{eC}}\right] \tag{9}$$

Neglecting back emission equation (8) becomes:

$$\frac{J_s}{J} = \exp\left[\frac{V_C}{kT_{eC}} - \frac{V_E}{kT_{eE}}\right] - \exp\left[\frac{-V_E}{kT_{eE}}\right] + 1$$

$$+ \frac{3}{4v}(\Sigma_1 + \Sigma_2)\, d \exp\left[-V_E/kT_{eE}\right] \tag{10}$$

From the motive of Figure III-1 we get:

$$V_E = \phi_E - \phi_C + V_C - eV \tag{11}$$

Substituting (11) in (10) results in:

$$\frac{1}{J} = \frac{1}{J_s} + K \exp\left[\frac{eV}{kT_{eE}}\right]\left\{\frac{3}{4v}(\Sigma_1 + \Sigma_2)\, d + L\right\} \tag{12}$$

where

$$K = \frac{1}{J_s} \exp\left[-\frac{\phi_E - \phi_C + V_C}{kT_{eE}}\right] \tag{13}$$

$$L = \exp\left[\frac{V_C}{kT_{eC}}\right] - 1 \tag{14}$$

Equation 12 shows that $\frac{1}{J}$, the inverse of the net electron current, is a linear function of the interelectrode spacing d. The proportionality constant depends

on the macroscopic cross sections of cesium and argon.

The dependence of equation 12 is shown graphically in Figure III-2. $\frac{1}{J}$ is plotted versus d for various values of output voltage V_1, V_2, etc. The solid lines correspond to a cesium vapor plasma, while the dashed line represents the case of cesium and inert gas acting simultaneously. These lines converge to a focal point whose d coordinate is a function of the macroscopic scattering cross section of the single or double vapor system. The $\frac{1}{J}$ coordinate is equal to $\frac{1}{J_s}$, the inverse saturation current. It is, therefore possible by plotting experimental data in this fashion to determine the increase in scattering due to argon atoms.

3. EVALUATION OF PLASMA PARAMETERS

More information can be extracted from experimental data by differentiating equation (12) with respect to d to obtain:

$$m = \frac{\partial (1/J)}{\partial (d)} = \exp\left[- \frac{\phi_E - \phi_C - eV}{kT_{ee}} \right] \frac{3}{4v} \Sigma_1 + \exp\left[- \frac{\phi_E - \phi_C - eV}{kT_{ee}} \right] \frac{3}{4v} \frac{V}{kT_g} \sigma_2 P_2 \qquad (15)$$

In equation (15) Σ_2 has been replaced by:

$$\Sigma_2 = N_2 \sigma_2 = \frac{V P_2}{kTg} \sigma_2$$

where N_2, σ_2 and P_2 are the density, microscopic scattering cross section and partial pressure of argon atoms in the interelectrode space respectively. T_g represents the gas temperature and V is the volume of the diode.

It is clear from equation (15) that if m is measured for several pressures of argon, a plot such as Figure III-3 can be constructed and electron temperature and the cross section σ_1 or σ_2 can be determined from the slope and the intercept.

By analyzing the experimental data using plots such as Figure III-3, it is possible to test the theory in a definitive way. The value of this test results from the fact that it is a direct measure of the effect of inert gas pressure. The use of inert gas provides an additional method of studying plasma parameters such as electron temperature, scattering cross sections and collector and emitter sheath heights.

Experimental data are presently being generated for specific use with the analytical tools developed. Typical families of current voltage curves are shown in Appendix A.

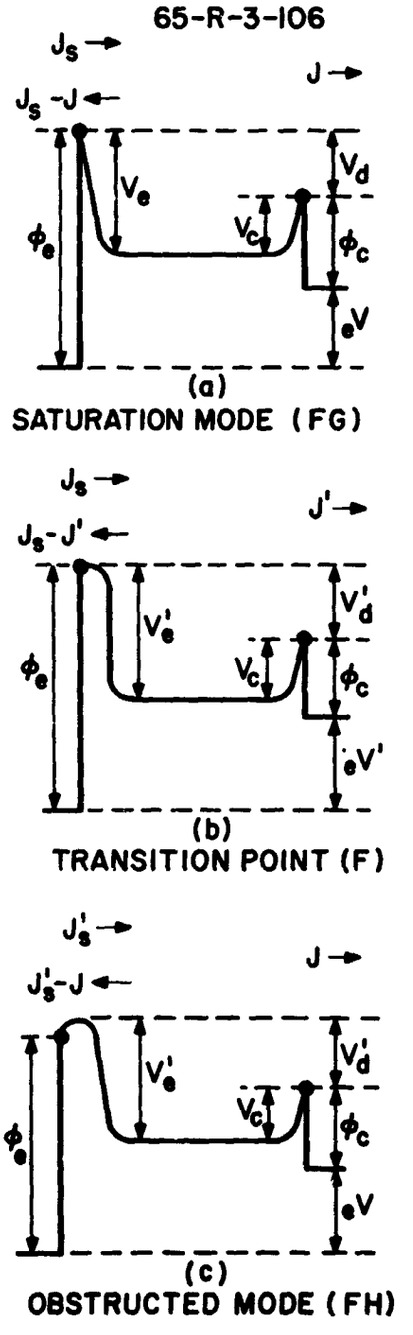

Figure III-1. Modes of Discharge

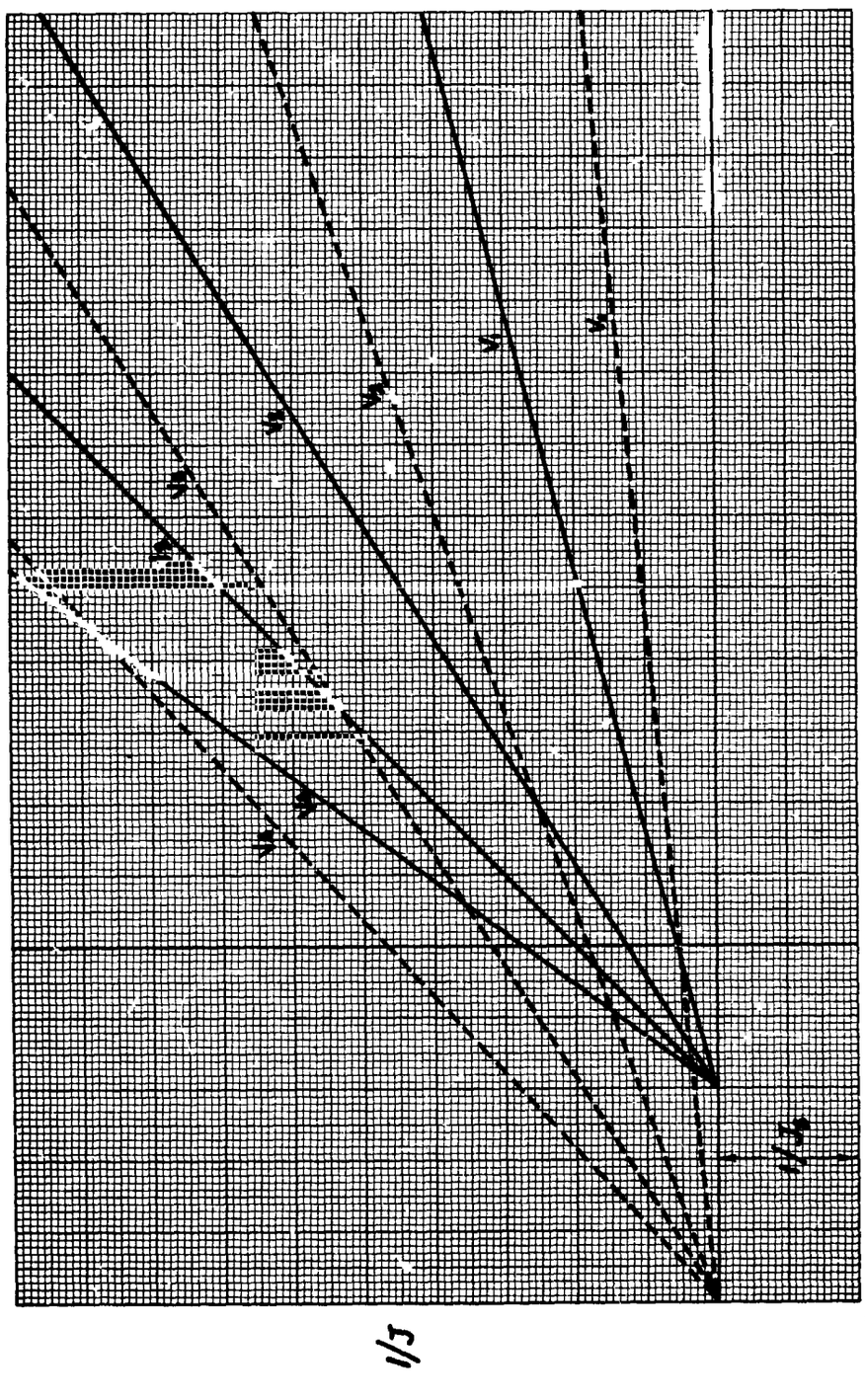

Figure III-2. Plot of Volt Ampere Characteristics According to Equation 12.

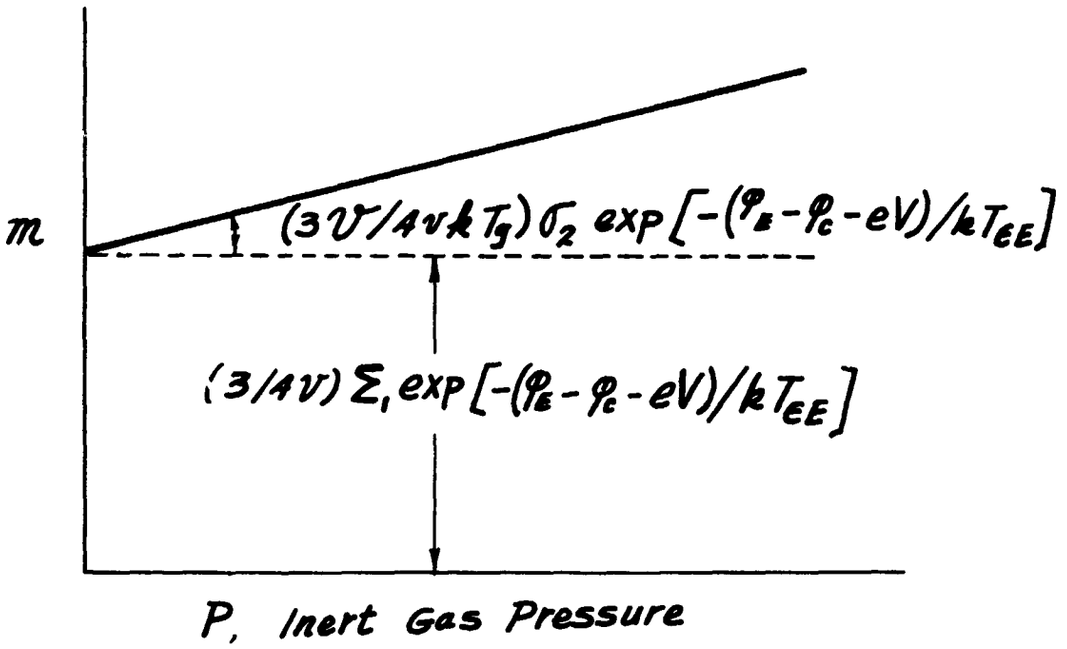

Figure III-3. Plot of Equation 15.

CHAPTER IV
SURFACE ADDITIVES

In the course of this program and in previous work a considerable volume of data pertaining to the system W - CsF - Cs has been accumulated. The task of analyzing and correlating these data has also progressed concurrently with the experimental task. As a result of these efforts a framework is emerging which allows the phenomenological description of this system in spite of the fact that many questions still remain unanswered. In this chapter this framework is presented and wherever possible the hypotheses advanced are tested with available experimental results.

The ultimate objective of the surface additive studies is to formulate a detailed model of the tungsten surface covered with fluorine, or any other electronegative element, and cesium. To successfully complete this task, additional experimental work is required. However, as an interim approach, the possibility of considering the tungsten surface with a fixed fluorine coverage as a metal with higher bare work function and then using the Rasor-Warner[1] theory to predict the cesiated work function was investigated and proved successful. This result, apart from its value as an aid in correlating experimental observations, is of fundamental significance because it implies that the effects of electropositive and electronegative adsorbates acting concurrently are separable in terms of their individual effects. The dynamics of additive desorption have been considered and a relation between fluoride coverage, surface temperature and arrival rate is presented. Finally, using a simple electrostatic model, the fluoride arrival rate required for a given work function change for low fluorine coverages is derived.

1. THE INTERDEPENDENCE OF Cs AND ADDITIVE EFFECTS

The Rasor-Warner analysis considers the two component system Cs - emitter surface, postulates a physical model for the surface and develops certain relationships

among the properties of the system. The present analysis proposes to apply the conclusions of the Rasor-Warner theory to the three component system Cs - electronegative element - emitter surface. To do this, the hypothesis is made that at constant additive coverage the additive - emitter portion of the system is equivalent to an emitter with a bare (non-cesiated) work function value equal to that obtained when the additive is the only adsorbate.

Rasor and Warner give the following expression for $\Delta\phi$, the change in work function of a metal surface when covered with an adsorbate:

$$\Delta\phi = \frac{1}{1-f}\left(\phi_o + \phi_{io} - I - T/T_R\, h - kT\,\ell n\, B/C\right) \qquad (1)$$

where: f is a fraction of the dipole layer potential drop penetrated by the ion core of the ad atom; ϕ_o-the normal bare electrode work function; ϕ_{io}-the image force binding the ad atom to the bare surface; I - the ionization potential of the ad atom; T_R - the ratio of surface temperature, T, to cesium reservoir temperature T_R; h - an activation energy for the evaporation of cesium from the reservoir and B and C are constants describing the desorption from the surface and evaporation from the reservoir respectively and are only slightly dependent on temperature. In this relation all the terms except the last two are practically independent of temperature and the equation may be simplified to:

$$\Delta\phi = A(\phi_o + D - h\,T/T_R - kT\,\ell n\, B/C) \qquad (2)$$

in the region of most interest in thermionic converters. Furthermore the last term may be neglected since the constants B and C are practically equal so that $\ell n\, B/C \approx 0$. It is possible, then, to relate the T/T_R values which will result in the same work function change $\Delta\phi$ for two materials which differ in bare work function by a given amount. Let the bare work function of the reference material be ϕ_o and its change in work function be $\Delta\phi$ for a surface to reservoir temperature

ratio T/T_R. Now, consider a material with bare work function equal to $\phi_o + \delta\phi_o$ and assume that it exhibits a change of work function equal to the reference $\Delta\phi$ at a new ratio $(T/T_R)'$ then it follows from equation (2) that

$$\phi_o + \delta\phi_o - h\,(T/T_R)' = \phi_o - h\,T/T_R \tag{3}$$

Or, the ratio of surface to reservoir temperature required to produce the same work function change in the new material as in the reference material is given by:

$$(\frac{T}{T_R})' = T/T_R + \frac{\delta\phi_o}{h} \tag{4}$$

h for cesium is 0.76 eV, substituting this value in (4),

$$(\frac{T}{T_R})' = \frac{T}{T_R} + 1.32\ \delta\phi_o \tag{5}$$

The work function value ϕ' corresponding to $(T/T_R)'$ is given in terms of the properties of the reference material by:

$$\phi' = \phi + \delta\phi_o \tag{6}$$

Using these relations and a ϕ versus T/T_R plot for tungsten and cesium a new plot of the straight line portion may be constructed for an additive covered surface knowing the $\delta\phi_o$ for a given additive coverage.

Measurements taken during the quarter have shown the additive to increase the bare tungsten surface work function by 0.4 to 0.7 eV depending on coverage. The most stable value being about 0.4 and the maximum 0.7 eV. Figure IV-1 shows the ϕ vs T/T_R curve for a ϕ_o of 4.62 eV corresponding to tungsten. The two dotted lines show the shift expected for $\delta\phi_o$ of 0.4 and 0.7 eV determined by the procedure outlined above. Experimentally determined work function values for tungsten in the presence of additive and cesium are shown as points in this figure.

Each group of points corresponds to a different emitter temperature.

These points give excellent agreement with the calculated curves in the higher T/T_R region showing that at the low Cs coverages the additive modifies the surface to produce a behavior equivalent to that of a pure surface of the same bare work function. At the higher coverages however, the curves do not bend as rapidly but continue towards lower work function values.

This deviation is most probably a limitation of the Rasor theory rather indicative of additive behavior since it has been observed in non-additive systems as well.

2. THE RATE-EQUILIBRIUM AND COVERAGE RELATIONS FOR ADSORBED ADDITIVES

The rate of desorption of particles adsorbed on a surface is governed by the Arrhenius equation:

$$\frac{dn}{dt} = A\,n\,e^{-E^*/kT_E} \tag{7}$$

where: n is the concentration of the adsorbed layer, dn/dt is its time rate of change, A a frequency factor, E* the activation energy for the process, k the Boltzmann constant and T_E the emitter temperature. To maintain a constant concentration, n, it is necessary to provide an arrival rate μ equal to dn/dt. Defining coverage, θ, as $\theta = \frac{n}{N}$ where N is the total number of available sites, the coverage is given by

$$\theta = \frac{\mu}{AN} e^{E^*/kT_E} \tag{8}$$

At very low additive coverages, it is possible to neglect the interactions of adsorbed additive particles and consider only the interactions between adsorbate

and substrate. This amounts to ignoring the depolarization of additive dipoles resulting from the field of adjacent dipoles. The value of the dipole due to the adsorbed layer is given by:

$$\chi = 4\pi\sigma r_1 q \tag{9}$$

where σ is the surface charge density, r_1 the effective distance in this case the covalent radius, and q the electronic charge, in cgs units 4.77×10^{-10}. The covalent radius of fluorine is given in reference (2) as 0.7×10^{-8} cm. Assuming that at full coverage one fluorine atom is adsorbed for every tungsten atom, σ will be set equal to the value of N reported by Langmuir of 4.8×10^{14} atoms/cm^2. Substituting these values in (11),

$$\chi = 6.15 \text{ volts} \tag{10}$$

$\delta\phi_{max}$, the change in work function that would result from a monolayer of fluorine in the absence of depolarization, is equal to the dipole layer potential, $\delta\phi_{max} = 6.15$ eV. At low coverages when in fact depolarization is absent, the change in work function is proportional to coverage:

$$\delta\phi_o = \delta\phi_{max}\,\theta = \frac{\delta\phi_{max}\mu}{AN} \exp\left[E^*/kT_e\right] \tag{11}$$

Statistical theory predicts an approximate value for the frequency factor A in terms of Boltzmann's and Planck's constants $A = kT/h = 10^{11}$ sec^{-1}. The activation energy E* can be calculated from measurements of the time constant for desorption. Such measurements have been conducted with CsF by Aamodt [3] and this laboratory.[4] In both cases, the activation energy values computed are about 145 K cal/g atom. Equation (11) was used to compute the arrival rate required to maintain a given coverage as a function of emitter temperature.

Figure IV-2 is a plot of the resulting family of curves. The CsF reservoir temperature corresponding to a given arrival rate is also shown.

In conclusion, it is possible to predict the thermionic properties of the three component system W - CsF - Cs from the plots of Figures IV-1 and IV-2. It should be noted that the relationships derived are still tentative and subject to further experimental confirmation.

CHAPTER IV

REFERENCES

(1) N. S. Rasor, C. Warner, Journal of Applied Physics, Vol. 35, p. 2589, 1964.

(2) L. Pauling, Nature of the Chemical Bond, Cornell University Press, p. 228, 1960.

(3) L. L. Aamodt, L.J. Brown and B. D. Nichols, Journal of Applied Physics, Vol. 33, p. 2080, 1962.

(4) S. Kitrilakis, F. Rufeh, D. Lieb, et al., Final Report Thermionic Research Program, Task IV, Contract No. 950671, Chapter VIII.

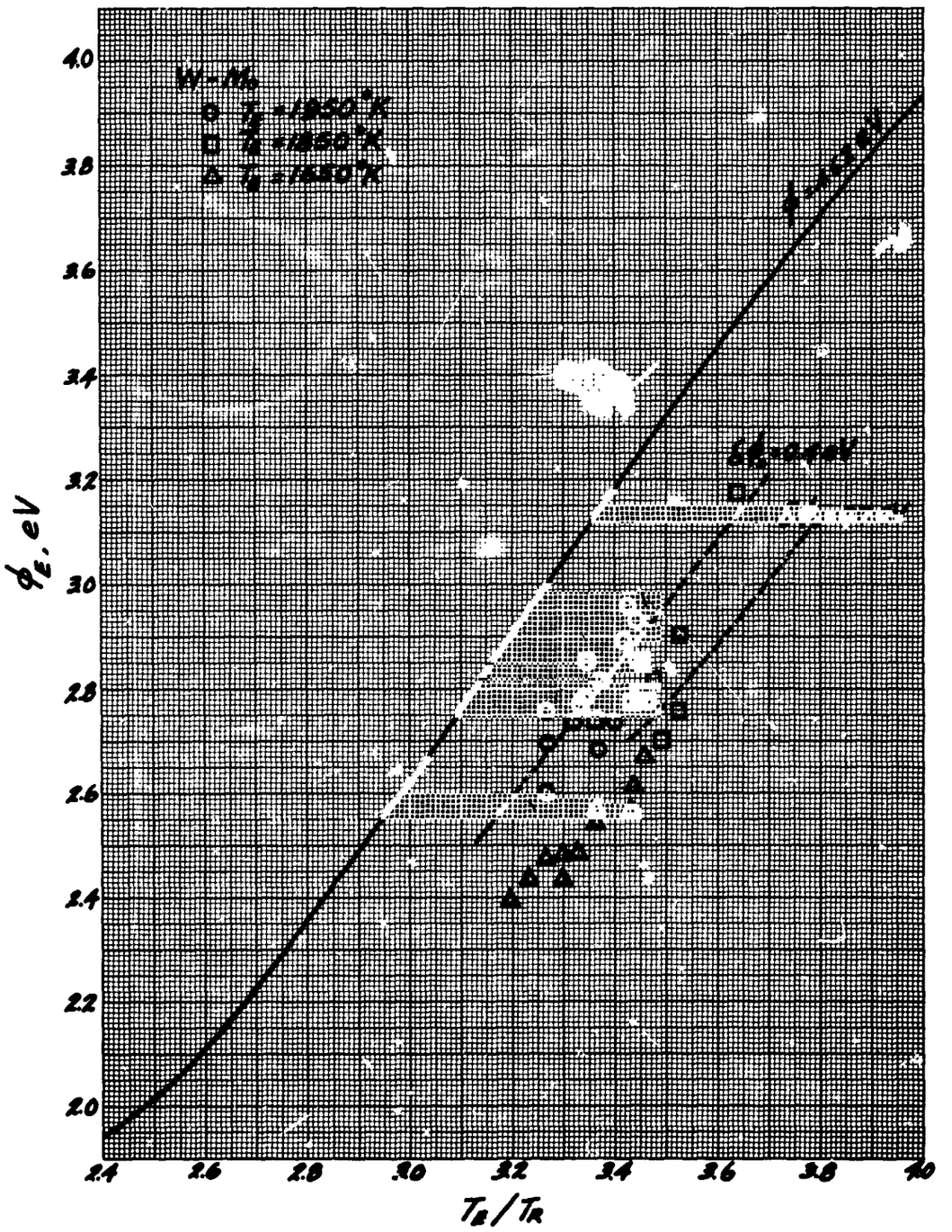

Figure IV-1. Emitter Work Function versus T_E/T_R for Cs and CsF.

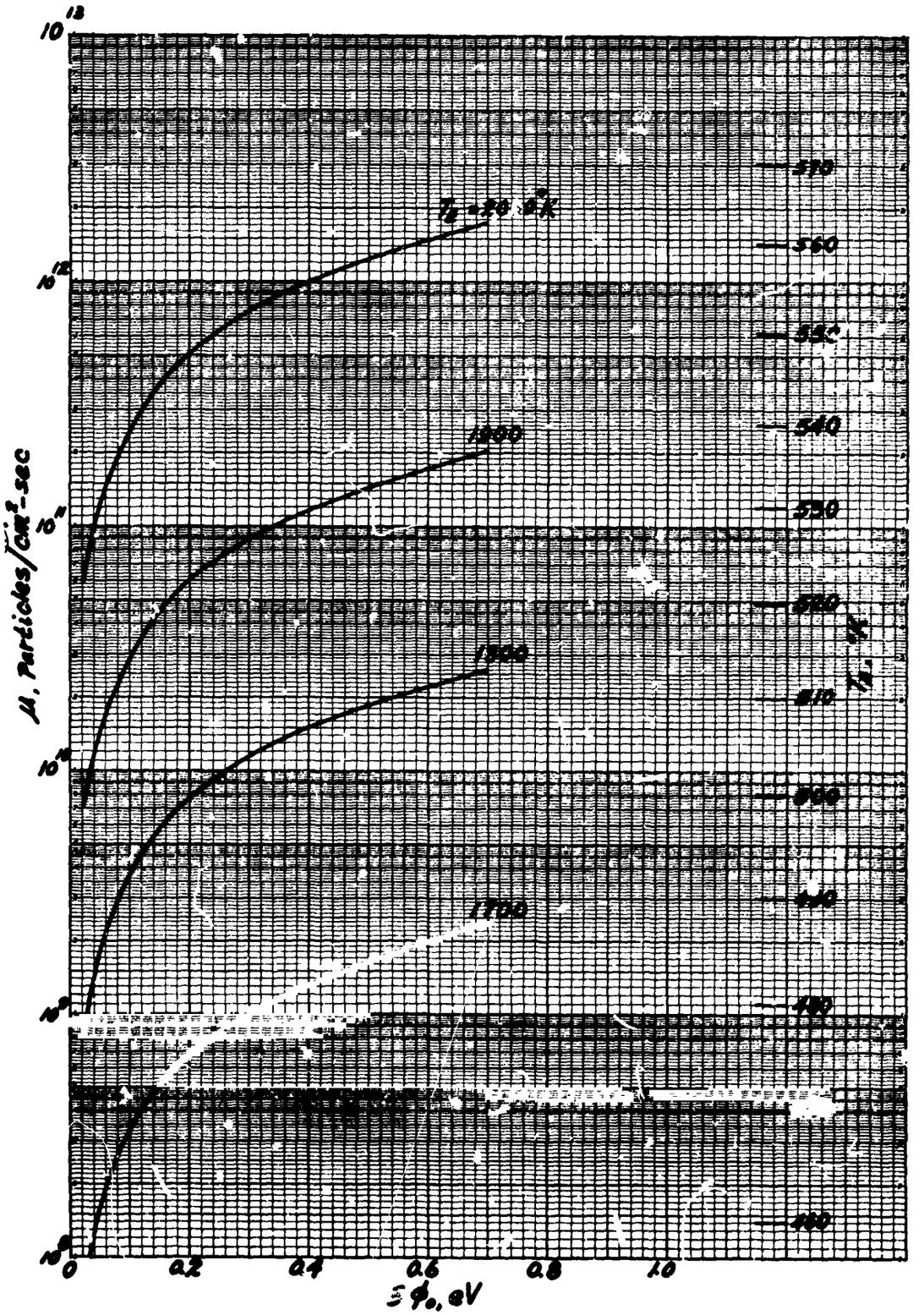

Figure IV-2. Effective Uncesiated ϕ_E as a Function of CsF Arrival Rate, T_E and T_A.

CHAPTER V

PLANS FOR NEXT QUARTER

During the third quarter of the program, the study of inert gas interactions with the cesium plasma will continue through both basic experiments and parametric studies. Particular emphasis will be placed on the interpretation of experimental results according to the hypotheses advanced in this report.

The surface additive task is expected to make significant progress toward removing certain ambiguities regarding additive behavior which still exist.

The theoretical effort during this quarter will be concentrated on the formulation of a detailed model for the adsorption of CsF on tungsten.

APPENDIX A

Typical variable cesium temperature families obtained to evaluate the overall effects of inert gases in cesium plasma.

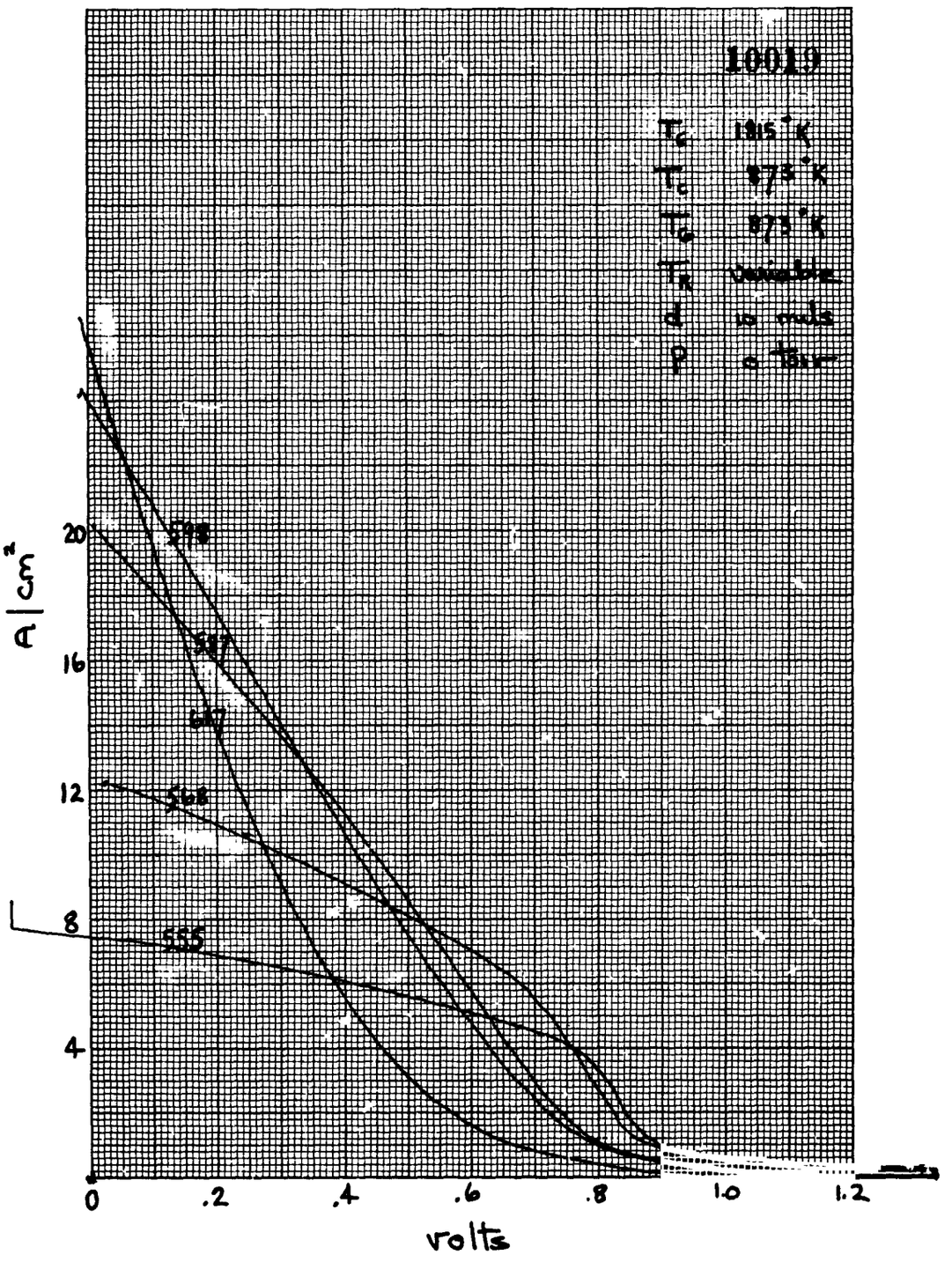
10019
T_e 1815°K
T_c 873°K
T_b 873°K
T_R variable
d is mils
P < 10^{-8} torr
A/cm²
20
16
12
8
4
0
.2
.4
.6
.8
1.0
1.2
volts
555

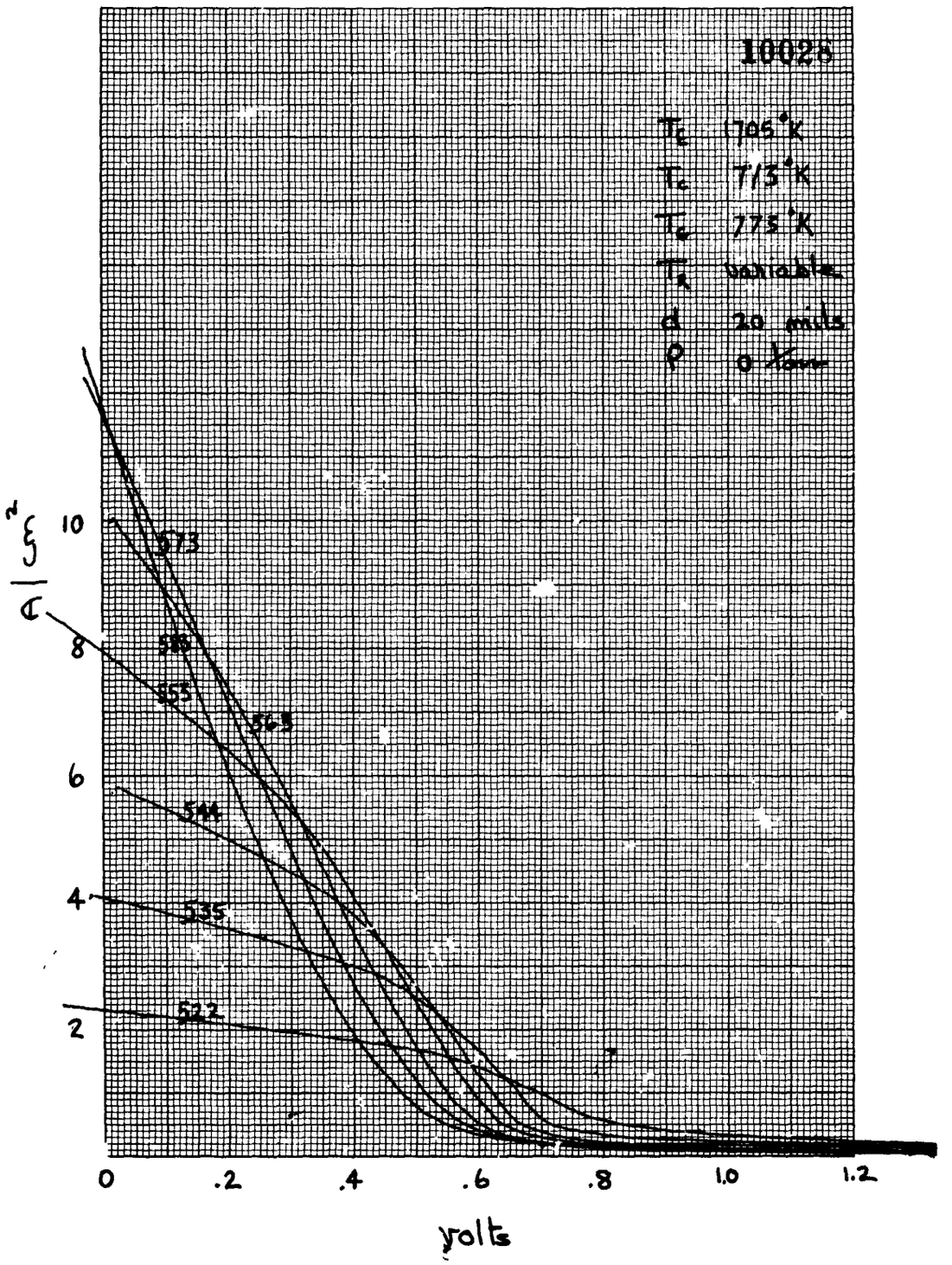
10028
T_E 1705°K
T_C 713°K
T_C 775°K
T_K variable
d 20 mils
P 0 Torr
$\frac{\xi}{\epsilon}$
10
8
6
4
2
573
555
565
544
535
522
0
.2
.4
.6
.8
1.0
1.2
volts

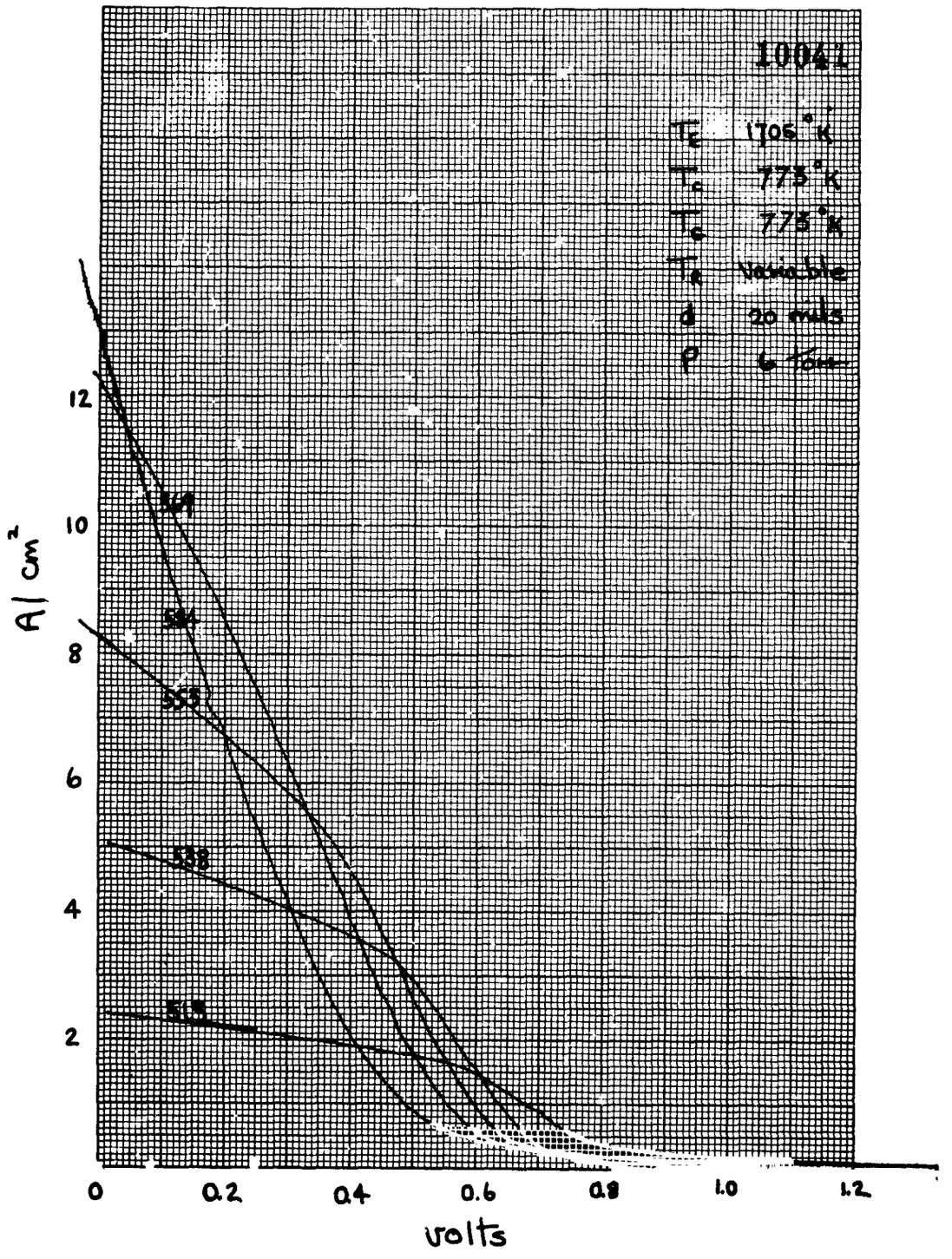
10041
T_E 1705°K
T_c 775°K
T_c 775°K
T_R Variable
d 20 mils
P 6 Torr
12
10
8
6
4
2
A/cm²
0
0.2
0.4
0.6
0.8
1.0
1.2
volts

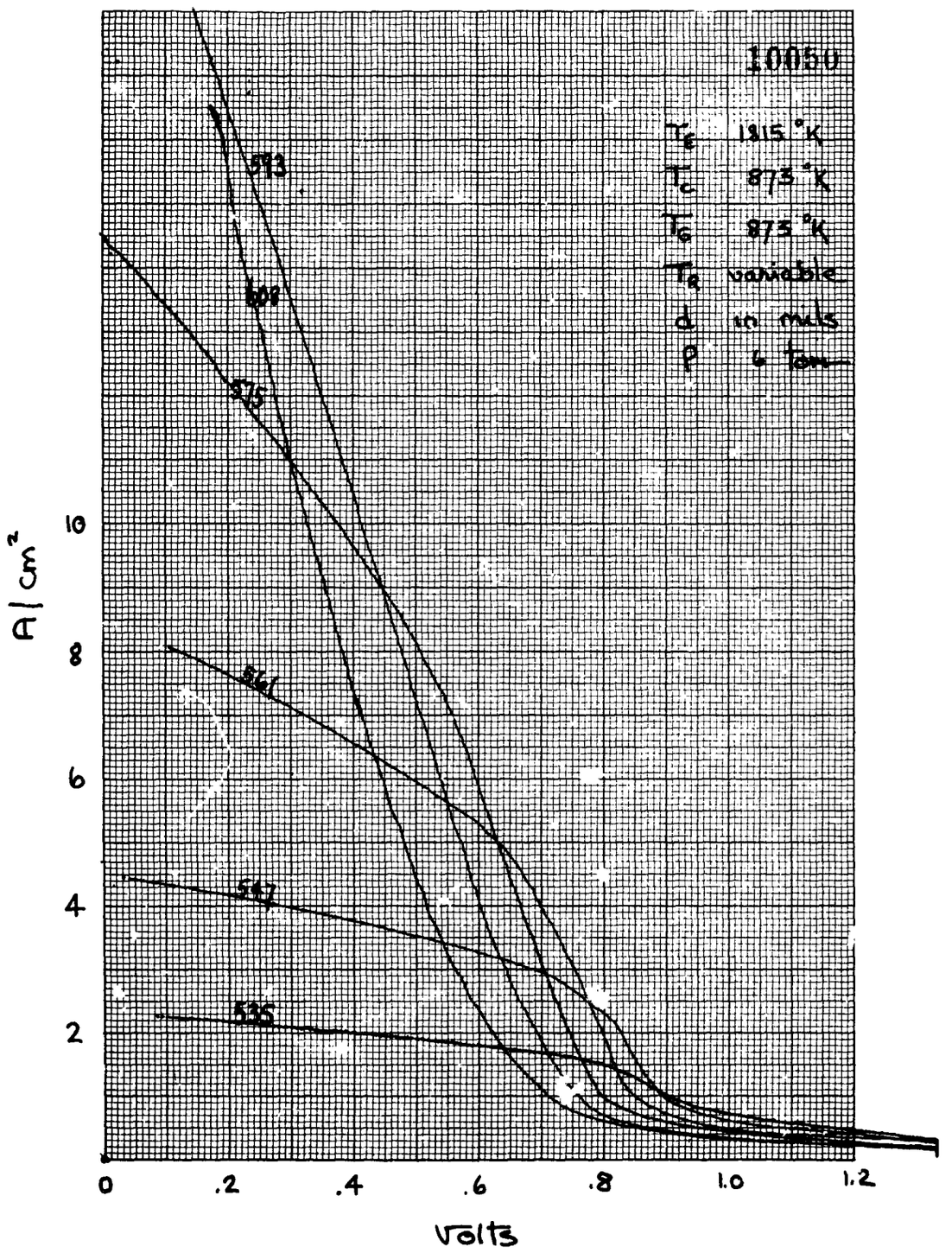
10050
T_E 1315 °K
T_C 873 °K
T_G 873 °K
T_R variable
d in mils
P 6 torr
913
806
575
861
547
535
A/cm²
10
8
6
4
2
0
.2
.4
.6
.8
1.0
1.2
Volts